EISSN: 2707-0425

East African Journal of Science, Technology and Innovation, Vol. 4 (Issue 4): September 2023

The correlation between equatorial electrojet and equatorial ionisation anomaly over the East African region during the solar minimum period 2008-2009

[1]MILIMU H., [1]OMONDI G., [2]MUNGUFENI P*

[1]Department of Physics and Materials Science Maseno University, P.O. Box 333-40105, Maseno-Kenya,
[2]Department of Physics, Muni University P.O. Box 725, Arua- Uganda.

***Corresponding Author:** hanningtonamilimu@gmail.com

Abstract

This study analyzed the correlation between the equatorial electrojet (EEJ) and the occurrence of equatorial ionisation anomaly (EIA) over the East African region. The study was carried out during both geomagnetically quiet and disturbed conditions when Kp index values were < 2+ and > 5+, respectively. The EEJ data were obtained using a pair of magnetometers located at Adis Ababa (geographic 9.04°N, 38.77°E, geomagnetic 0.17°N, 110.47°E) and Adigrat (geographic 14.281°N, 39.46°E, geomagnetic 6.0°N, 111.06°E), both in Ethiopia while the EIA data were derived from the total electron content (TEC) data that were obtained using a set of Global Navigation Satellite System (GNSS) receivers within the East African region. The data used were for the years 2008 and 2009. The TEC data over the crest of EIA were divided by those over the trough to quantify EIA strength over the region. The EEJ intensity was estimated from the difference in the horizontal component of the geomagnetic field observed by the pair of magnetometers. The results during quiet geomagnetic conditions showed that peak values of EEJ which range from 48nT - 110nT occurred between 10:00 and 14:00 LT. The EIA's peak which varies from 1.20 to 1.45 occurs between 20:00 to 22:00 LT. The correlation coefficients were found to vary from moderate (0.58) to strongest (0.74). During geomagnetically disturbed conditions, the correlation coefficient ranges from 0.28 to 0.45. The increased eastward electric field and photo-ionization on TEC are responsible for the strong link between EEJ and EIA. This study reveals the trend in the variation of the strength of EEJ and EIA over the East African region which can be used as a basis for developing regional models to forecast or nowcast scintillations and the ionospheric space weather prediction over this region.

Keywords: *Equatorial Electrojet, Equatorial Ionization Anomaly, Total Electron Content, Quiet geomagnetic condition, disturbed geomagnetic condition*

Received: 09/05/23
Accepted: 04/09/23
Published: 29/09/23

Cite as: *Milimu et al, (2023)* The correlation between equatorial electrojet and equatorial ionisation anomaly over the East African region during the solar minimum period 2008-2009. *East African Journal of Science, Technology and Innovation 4(4).*

Introduction

The Equatorial Electrojet (EEJ) is a narrow band of enhanced eastward current flowing in the E-region (100-120km) altitude within ±2° at the geomagnetic equator (Chakraborty & Hajra, 2009; Lühr et al., 2021). The Equatorial Ionization Anomaly (EIA) is another feature of the equatorial and low-latitude ionosphere and it belongs to the outcome of the ion continuity equation. EIA can be described as the plasma redistribution between the hemispheres, resulting in a low latitude peak in each

hemisphere and reduced plasma (trough) marginally above the dip equator in each hemisphere (Yamazaki et al., 2014).

The radio waves that traverse the ionosphere experience intermittent amplification and fade called scintillations due to ionospheric irregularities caused by intricate physical phenomena in the solar-terrestrial environment. When these scintillations are strong, they affect navigation and communication systems (Eastes et al., 2019). It is important to note that ionospheric irregularities commonly occur over the EIA region.

Through low solar activity years, it is assumed that ionospheric conditions are almost constant with respect to time due to the low rate of ionization. However, during and after a high solar activity period, ionospheric conditions change very rapidly. Throughout the eleven-year solar sunspot period, the frequency of geomagnetic disturbance varies, becoming more common as sunspot counts increase. The sun undergoes an alternating radiation cycle of around eleven years, called the solar (sunspot) cycle. The ionosphere has a larger electron density when compared to other times during solar maximum periods (most sunspots).

Research has been done to understand the EEJ's effect on the development of the EIA. This is due to significant changes in electron concentrations from both sides of the magnetic equator affecting signals of the ionospheric radio frequency and communication systems with the ground-to-ground high-frequency. For instance, Rabiu et al., (2017) built an empirical model of the EEJ magnetic signature, including local time and longitudinal dependence, based on concurrent measurements made at 12 magnetometer stations spread across six distinct longitude sectors. They then normalized the observation data to the dip equator. The investigation revealed that between 09:00 and 10:00 LT, the EEJ component was strongest in the South American sector and weakest in the Indian sector, but from 11:00 to 14:00 LT, it shifted to the African sector. In order to find trustworthy precursors of the occurrence of ionospheric anomalies, Dabas et al., (2003) used ionosonde data from ground-based observations to carry out the study on the strength of EEJ in the Peruvian sector. They noticed that along the magnetic equator, the EEJs are seen intensified and centered around local noon. In comparison to solstice months, equinox months have a greater local noontime EEJ intensity. On the other hand, Balan et al., (2009) reviewed the EIA and the ionospheric irregularities. It was observed that the EIA develops in the morning, continues to exist well beyond the sunset, and covers up to half the global area in 24 hours. But since the dynamics of the ionosphere depends on various factors including the solar cycle, both geomagnetic quiet and disturbed conditions, geographical locations and time, and also most of the EEJ and EIA studies have been conducted on Indian and American region, this study will focus on the EEJ and EIA correlation in the East African region.

The correlation between EEJ and EIA is necessary since EEJ is one of the systems responsible for the plasma uplift in the equatorial regions thereby generating Equatorial Ionization Anomaly, which indicates a linkage between EEJ and EIA. Therefore, much research has been conducted to understand this linkage. The knowledge gaps identified by this study are that correlations have not been done during geomagnetically disturbed and quiet conditions, it is necessary to get a complete picture for both geomagnetically disturbed and quiet conditions.

The East African sector was chosen as a study region since the studies done over this region were during the time of increased solar activity (Rush et al., 1969; Mungufeni et al., 2018). Therefore, we have limited knowledge of the link between the EEJ and the EIA development in the East African region when the sun is at its lowest. This research performed the correlation between EEJ and EIA during the years 2008 and 2009 over the East African region. These are solar minimum years in sunspot cycle 23. Some of the magnetometers over Ethiopia were not operational in solar minimum years 2019 and 2020 in sunspot cycle 24. Currently, we are in the ascending phase of sunspot cycle 25.

In the next section, the materials and methods of the study are discussed.

Materials and methods

Data and region of study

The region of study is East Africa. In this study, the data used were obtained from the East African longitude sector bounded by geographic 30 - 45°E longitude and -3.1 - 15°N latitude. The X, Y, and Z components of the Earth's magnetic field observed by the magnetometer at Adigrat (ETHI) were obtained from http://www.magnetometers.bc.edu while the same data set observed by magnetometer at Addis Ababa (AAE) (geographic 9.04° N, 38.77° E, geomagnetic 0.17° N, 110.47° E) were obtained from http://www.intermagnet.org both in Ethiopia. Moreover, the GNSS data that was saved in Receiver INdependent EXchange (RINEX) files, were used in this research. The list of station names, their codes, and geographical and geomagnetic coordinates used in this study are shown in Table 1.

Table 1

Table showing the GPS receiver stations used in this study

S/N	Station name/Country	Station codes	Geographic Lat. (°)	Geographic Lon. (°)	Geomagnetic Lat. (°)	Geomagnetic Lon. (°)
1.	Addis Ababa (Ethiopia)	AAB	8.97	38.75	0.17	110.48
2.	Adigrat (Ethiopia)	ETHI	14.28	39.46	6.00	111.06
3.	Nairobi (Kenya)	RCMN	-1.24	36.81	10.76	108.51
4.	Malindi, Kenya	MAL2	-3.10	40.10	-12.40	10.50
5.	Mbarara, Uganda	MBAR	- 0.60	31.00	- 10.76	17.30

The RINEX files were processed to obtain TEC data which were in turn used to derive information about EIA. On the other hand, the geomagnetic field observations at ETHI and ADIS were used to compute EEJ as in the next section. The stations under consideration have a limited latitudinal range in order to pinpoint the EIA trough and crest across the region. Both geomagnetically quiet days (Kp≤2+) and geomagnetically storm days data (Kp≥5+) were put into consideration.

Methodology

Estimation of the Equatorial Electrojet (EEJ) strength. The difference between the horizontal component (H) of the earth's magnetic field's magnitudes measured by magnetometers at ETHI (H_{SE}) and those estimated at AAE (H_{SA}) for the simultaneous days was used to determine the EEJ strength Venkatesh et al., (2015). An approximate measurement of the electrojet current during the day is the difference observed between the two horizontal components (Delta H) (Mungufeni et al., 2018).

Since magnetospheric currents have an impact on both ADIS and ETHI during the entire month, the baseline was therefore important to effectively eliminate the contributions of magnetospheric currents. The horizontal magnetic field was recorded 150 minutes before and after midnight on each day, and its arithmetic mean served as the baseline. The 300-minute flanking local midnight was chosen as a baseline since around that time the value was constant.

$$H_B = \frac{1}{300}\sum_{t=1}^{300} H_t \qquad 2.1$$

To account for various offset values of different magnetometers, the difference between the daily values of the baseline (H_B) and each of the sixty-second resolution H-field values was determined according to equation 2.2 (Yamazaki et al., 2014). The values that were obtained after subtracting H_B from H for a specific station were denoted as H_S (see equation 2.2).

$$H_s = H - H_B \qquad 2.2$$

To get the equatorial electrojet, the difference is obtained between the H_S values recorded at ETHI (H_{SE})and the values computed at AAE (H_{SA}) in accordance with equation 2.3 below.

$$EEJ = H_{SA} - H_{SE} \qquad 2.3$$

The results obtained using equation 2.3 can be found in Figures 1, 2, 3, 4 and 5.

Quantifying Equatorial Ionization Anomaly Strength.

The TEC is defined as the sum of integrated electrons along the path from the receiver (R) to the GPS satellites (S), mathematically written as,

$$\mathrm{TEC} = \int_R^S N_e\,(\mathrm{P_i})\mathrm{d}s_i\,, \qquad 2.4$$

where N_e is the total number of accumulated electrons in each square metre through the differential distance ($\mathrm{d}s_i$) along the path from the satellite to the receiver on the ground, p_i.

TEC is a parameter used to describe the ionosphere, usually expressed in TEC units (TECU) with 10^{16} electrons per square meter equivalent to 1 TECU. It can be determined from the phase delay or advance of GPS signals when they pass through the ionosphere. The nominal range is 10^{16} to 10^{19} electrons per square metre with minima and maxima occurring at night and the day, respectively. At night the TEC decays rather slowly due to the recombination of electrons and ions.

The RINEX observation files were downloaded from the ADIS, MAL2, MBAR, DEBK, MOIU, ARMI, NEGE, and RCMN, IGS from 1st January 2008 to 31st December 2009.

The software developed by Gopi Seemala was used to process the intended (CMN) output files. Data for all observable satellites and elevation angles are available in the CMN files. In order to exclude the impacts of multipath, only the data from satellites with elevation angles greater than 30 were used.

The data were analyzed as follows: The daily VTEC data were classified into months for all the days throughout the study period. As a result, 12 monthly bins were created for each year from the years 2008 to 2009 data. The monthly bins were classified further according to local time. The monthly average TEC with 30s resolution was calculated using the average values of the local time bins. To quantify the EIA, the TEC values at the crest were divided by those at the trough, yielding the crest-to-trough TEC ratio (CREST: TROUGH ratio). The results obtained are represented in Figure 3. The benefit of the CREST: TROUGH ratio over other approaches (Calculating the difference between the TEC obtained at the peak and that measured at the trough, estimating the normalized difference between the crest's TEC and the trough's TEC, and using the obtained TEC at the crest's peak directly) is that it offers a relative variation of the EIA, which is typically effective at illustrating variation in physical phenomena (Yue et al., 2014).

Figure 1

Average EEJ against local time during geomagnetically quiet days in 2008

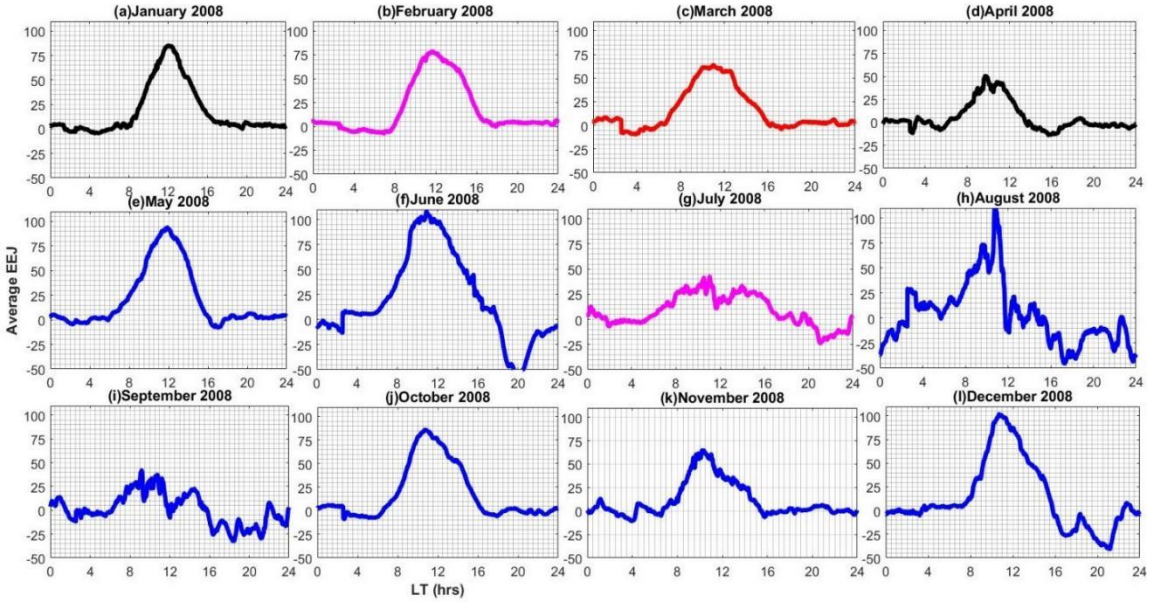

Figure 2

EEJ against local time during the geomagnetically disturbed day in September 2008 and July 2009

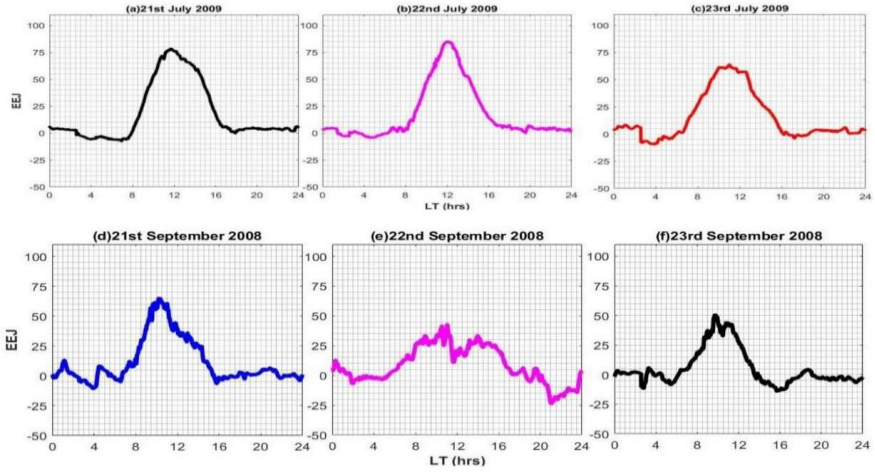

Figure 3

EEJ against local time during the geomagnetically disturbed day in March and June 2008.

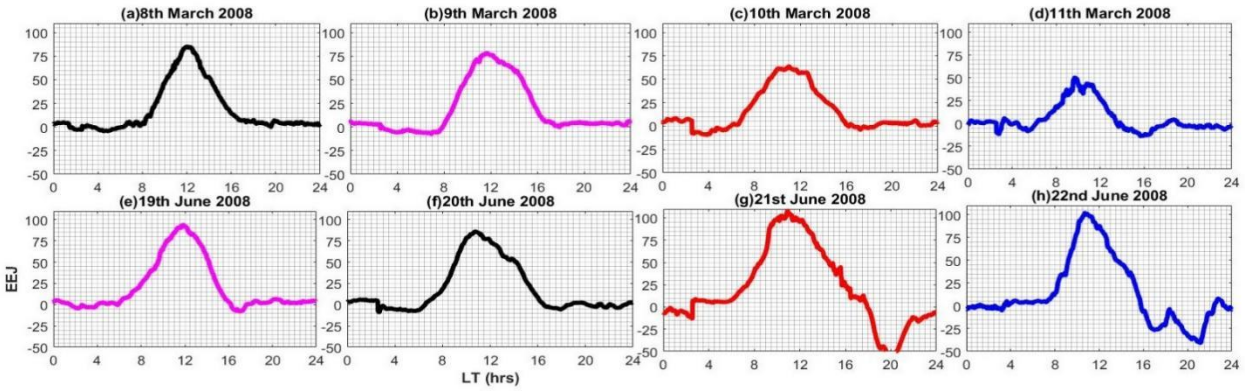

The analysis of the correlation between EEJ and EIA

Correlation is a quantitative measure that indicates the extent to which two or more data sets fluctuate in relation to each other. The correlation coefficient, on the other hand, is a statistical indicator of the strength of the linear link between two variables. There are different types of correlation coefficients. In this study, Pearson's correlation coefficient was used since it allows for strong inferences. It is parametric and measures linear relationships. This means that it provides data on both the strength and the direction of the link.

The correlation between EEJ and EIA was required since EEJ is one of the systems that lift plasma in equatorial regions, causing Equatorial Ionization Anomaly, which suggests a connection between EEJ and EIA. As a result, extensive research has been done to comprehend this connection.

The EEJ data were plotted against EIA to determine the correlation coefficient. The coincident values plotted were those that correspond hourly. The values plotted were picked after every three hours from midnight. The times at which the EIA values were picked include 03:00 LT, 06:00 LT, 09:00 LT, 12:00 LT, 15:00 LT, 18:00 LT and 21:00 LT. The results of this correlation are found in Figure 5.

Figure 4

Average EIA against Local Time in hours at (a) Mbarara- Uganda, (b) Nairobi-Kenya and (c) Malindi-Kenya in 2008 during geomagnetically quiet days while (d) –(k) shows EIA against Local time in hours in Nairobi during geomagnetically disturbed days.

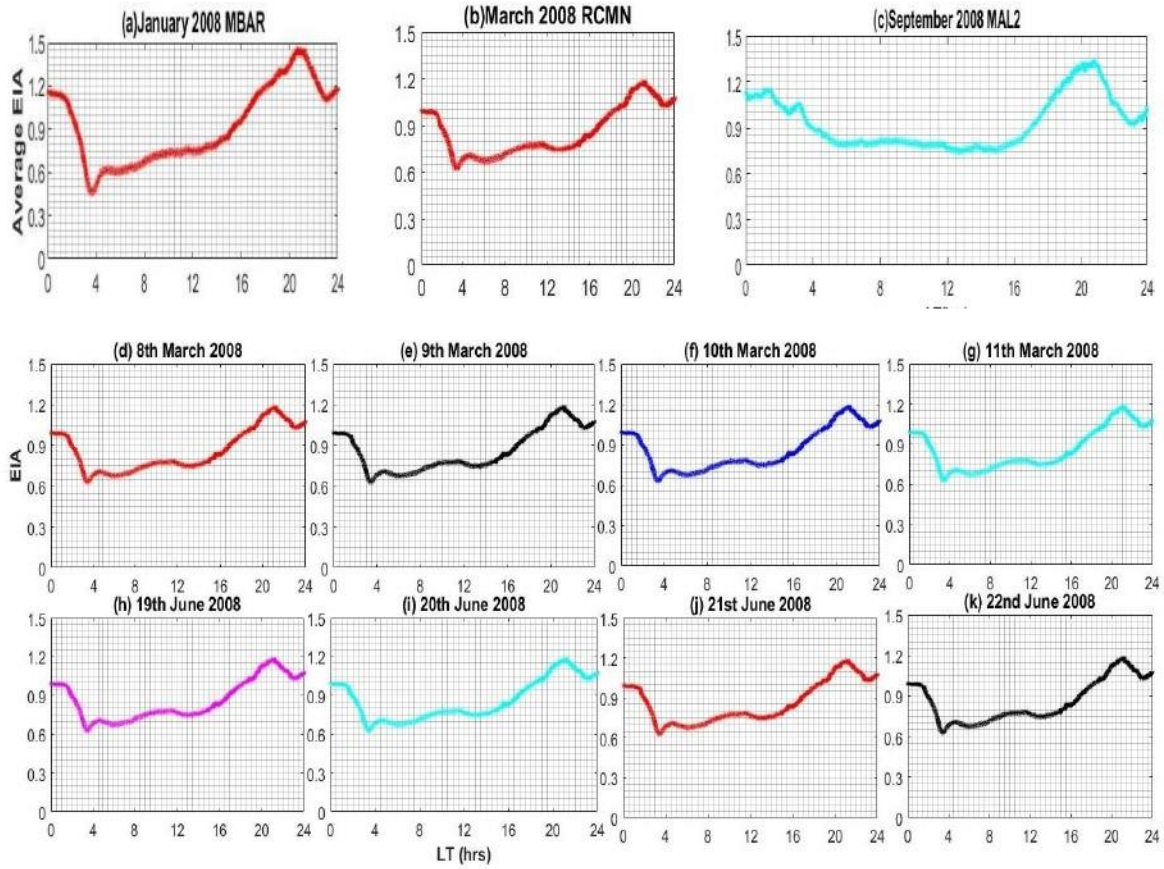

Figure 5

The EIA against EEJ in the following locations: (a) Malindi, Kenya, on a geomagnetically disturbed day in August 2008; (b) Mbarara, Uganda, on a geomagnetically quiet day in March 2009; (c) Nairobi, Kenya, on a geomagnetically quiet day in September 2008; and (d) Nairobi, Kenya, on a geomagnetically disturbed day in December 2009.

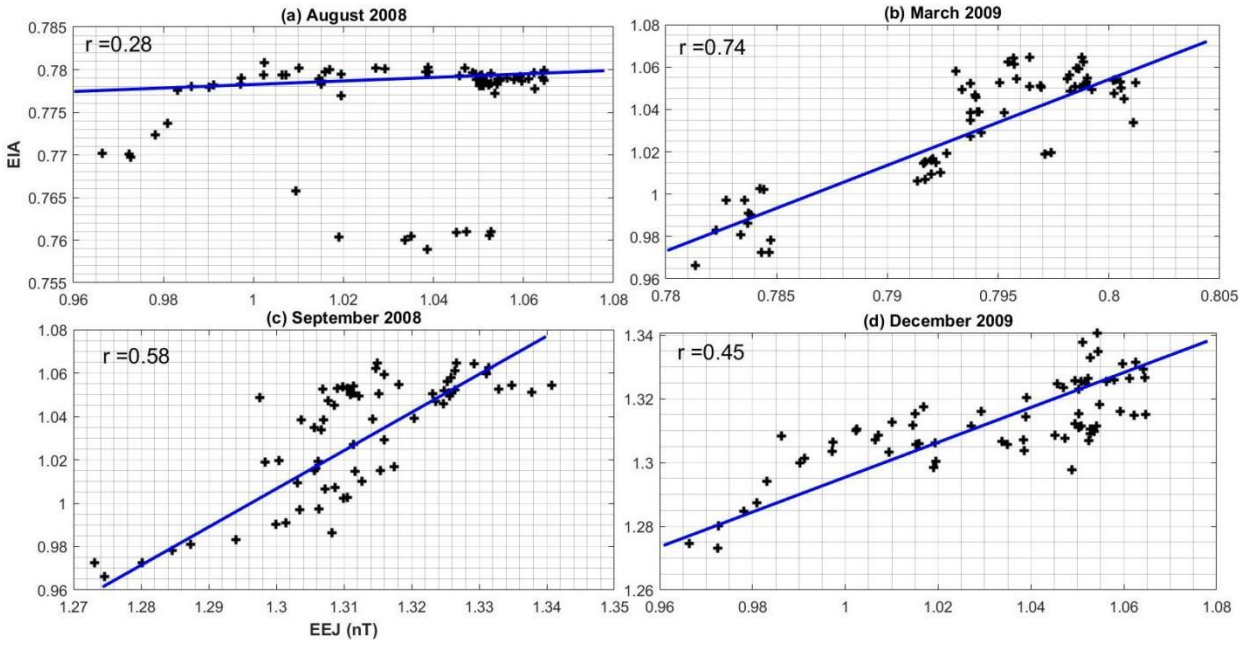

Results

The Equatorial Electrojet (EEJ) strength over the East African region

The EEJ on Geomagnetically Quiet Days

The EEJ for the quiet days during the study period was calculated using equation (2.3). The results are presented in Figure 1, panels (a) – (l). Figure 1 presents the average EEJ for the selected most quiet days from January - December 2008. From all panels in Figure 1, it is seen that the peak value of EEJ which ranges from 48 - 110nT occurs between 10:00 LT and 14:00 LT. It is also important to point out that the highest peak of EEJ occurred in August 2008 recording 110nT while panel (i) shows the lowest peak of EEJ (48nT) which was in September 2008.

The EEJ on Geomagnetically Disturbed Days

The geomagnetically disturbed days of 8th to 11th March 2008, 19th to 22nd June 2008, 21st to 23rd September 2008, and 21st to 23rd July 2009, when the Kp – index was ≥ 5, were considered. The EEJ during geomagnetically disturbed days was determined and the results are presented in Figures 2 and 3. As in Figure 1, the EEJ peak in Figures 2 and 3, also occurs between 10:00 and 14:00 LT. The EEJ's maximum value occurs at 10:00 LT in panels (a), (b) and (c) in Figure 3. From Figure 2, the peak value of EEJ on 21st June 2008 is much higher than any other value. The trough is observed on the 21st and 22nd of June 2008 as well as on the 21st, 22nd and 23rd of September 2008 in Figure 2.

Quantifying the strength of EIA during the solar minimum period over the East African sector

The EIA on Geomagnetically Quiet Days

The plots of Average EIA against Local Time in hours at Mbarara- Uganda, Nairobi-Kenya and Malindi-Kenya are presented in Figure 4 panels (a), (b) and (c) respectively. From Figure 4, the

EIA greater or equal to 1 was considered as the occurrence of EIA. This means TEC at the crest exceeds that at the trough.

The EIA begins building around 18:00 LT and lasts till 22:00 LT. In all the months of the year 2008, there is a certain instance of the EIA continuing past 23:00 and extending till 24:00 local time (see Figure 4, panels (a), (b) and (c)). Panels (a), (b) and (c) in Figure 4 show that the EIA troughs occur between 03:00 - 18:00 LT and 22:00 – 23:00 LT while the EIA crest occurs at 20:00 LT. The EIA troughs and crests are more prolonged in Mbarara compared to Nairobi and Malindi.

The EIA on Geomagnetically Disturbed Days

Figure 4 presents panels for geomagnetically disturbed days labeled (d) to (k). The EIA begins building around 01:00 LT and lasts till 24:00 LT in Figure 4, (d) – (k). These observations differ slightly from those on panels (a) to (c). There is a clear occurrence of the EIA crest in all the geomagnetically storm days at 20:00 LT (see Figure 4, (d) – (k)). The EIA crests are more prolonged in Mbarara compared to Nairobi and Malindi.

The presence of two crests in Figure 4 (d) to (k) is another significant trait worth noticing.

The correlation between EEJ and EIA

The scatter plots of EIA against EEJ during both geomagnetically quiet and disturbed conditions are presented in Figures 5 a. (Malindi, Kenya), b. (Mbarara, Uganda), c. and d both in Nairobi, Kenya. The analysis of the correlation was carried out and the correlation coefficients were obtained. The EIA was strongly correlated to EEJ in March 2009 in Mbarara, Uganda with a correlation coefficient of 0.74 (see Figure 5b) while Figure 5a (August 2008 in Malindi, Kenya) shows a weak positive correlation between EIA and EEJ with a correlation coefficient of 0.28. During geomagnetically disturbed conditions, the correlation coefficient ranges from 0.28 to 0.45. (See Figures 5a, b, c and d).

Discussion

The peak value of EEJ which ranges from 48 - 110nT occurs between 10:00 LT and 14:00 LT as recorded in Figure 1. Figure 1, panel (h) reveals that the highest peak of EEJ occurred in August 2008 recording 110nT while panel (i) shows the lowest peak of EEJ (48nT) was in September 2008. From Figure 2, the peak value of EEJ on 21st June 2008 which is much higher than any other value is associated with prompt penetration of electric field which increases ionization rates. When EEJ reverses direction, it's called counter electrojet (CEJ). The trough observed on the 21st and 22nd June 2008 as well as on the 21st, 22nd and 23rd September 2008 in Figure 2 is associated with CEJ occurrences in these months.

Also noteworthy is the fact that the EEJ peak on the storm days of March 9th and 22nd September 2008, was suppressed by the geomagnetic storm ring currents that are flowing westward. These results are consistent with those obtained by Jose et al., (2011) and Schnepf et al., (2018) for American, Brazilian and Japanese longitude sectors with the difference in the time of peak associated with the changes in the thermospheric wind.

These results for disturbed days clearly show the dependence of the intensity of the EEJ current on time and seasonal conditions. From Figure 2, there is an increase in EEJ peak at the start of the storm due to the sudden commencement of the storm and the prompt penetration electric field being present to the equatorial region, increasing ionization rates but later the EEJ is suppressed by the storm. The results differ from that of other studies done in India and some parts of American regions where the strength of the EEJ is weaker than in Equatorial regions. This variation is attributed to the change in longitude and latitude which varies from one region to another.

Because the EEJ peaks at noon, cases of substantial EIA 8 hours later are not as a result of rising zonal electric fields linked to higher EEJ. Other events, like the PRE just before this period, can be a contributing factor (Chau et al., 2015). Additionally, even though the fountain effect is primarily responsible for the EIA to form, neutral meridional winds at altitudes in the F region can have an impact on a variety of subtle aspects of the EIA morphology, according to Pedatella et al., (2014). The EIA recorded between 03:00 and 18:00

LT has a larger trough than the EIA recorded between 22:00 and 23:00 LT because of the extended fountain effect. In Malindi, the absence of January – May 2008 panels is due to the lack of data for these months across multiple stations. The lack of data would make it more difficult to observe EIA features over the area.

The presence of EIA across East Africa between 03:00 and 18:00 LT concurs with the findings of Sethia et al., (1980) and Klobuchar et al., (1990). On the other hand, our results during geomagnetically quiet days are different in some ways from those published by Bolaji et al., (2017) during geomagnetically quiet days in the low solar activity year of 2009. For example, their research showed that the EIA hardly occurs after 18:00 local time and that there is essentially no EIA activity beyond this hour. Their investigation showed a maximum TEC strength at the southern crest of about 50 TECU, whereas our results showed a maximum strength of about 45 TECU. The observed rise in electron density around the magnetic equator was caused by ionization brought on by the sun's position above the southern crest towards the zenith. In contrast, the EIA values rise during geomagnetically disturbed conditions since when plasma is carried far from the magnetic equator, the zonal electric field increases, causing the EIA to increase. The presence of two crests in Figure 4 (d) to (k) was also shown across the southern low- and mid-latitude areas of East Africa by Bolaji et al., (2017). Though, the identical feature that was noticed north of the magnetic equator was the focus of their attention. They proposed that the erratic transit of plasma to higher latitudes can cause these circumstances. To correlate EEJ and EIA it is important to note that all the geomagnetically quiet days in August 2008 and December 2009 with Kp ≤ 2+ in Malindi and Nairobi respectively were selected. All the days with Kp ≥ 5+ were also selected in Mbarara and Nairobi in March 2009 and September 2008. From Figures 5a, b, c and d, it can be concluded that the correlation coefficients were found to vary from moderate to strongest during geomagnetically quiet conditions, ranging from 0.58 to 0.74. During geomagnetically disturbed conditions, the correlation coefficient ranges from 0.28 to 0.45. (See Figures 5a, b, c and d). The rise in photo-ionization and the eastward electric field is responsible for the strong correlation between EEJ and EIA.

The coefficients calculated in the year 2008 are congruent with those computed using the 2009-related data (EIA and EEJ are strongly correlated during geomagnetically quiet conditions and weakly correlated during disturbed conditions).

From the p-values obtained during geomagnetically quiet conditions in Mbarara, Uganda and Nairobi, Kenya ($p = 0.02$ and 0.03), there is sufficient evidence to conclude that there is a statistically significance linear relationship between EEJ and EIA. This is because the p-values are less than 0.05 (0.02 and 0.03 values are far away from 0.05).

The main results obtained from the analysis are: (1) The local time of day, season, and solar activity have been found to have an impact on the amplitude of EEJ. The fluctuation in solar heating and ionization rates is what is responsible for this local temporal dependence. (2) The EIA starts accumulating from 01:00 LT and lasts until 24:00 LT. (3) The fountain effect is primarily accountable for the formation of the EIA (4) The EIA troughs and crests are more prolonged in Mbarara compared to Nairobi and Malindi. (5) The maximum EIA strength levels appear to occur between 18:00 and 22:00 LT. As mentioned earlier this is attributed to the prompt penetration electric field which increases ionization rates.

Conclusion

This study's objectives were to ascertain the EEJ's strength; quantify the strength of the EIA and analyze the correlation between EEJ and EIA from the year (2008) to the year (2009) within the East African region. This was done for both geomagnetically quiet and disturbed conditions. In a nutshell, the following are the main knowledge advancements made by the current study. (a) The peak value of EEJ occurs between 10:00 LT and 14:00 LT which can be attributed to the highest rate of ionization during this period. (b) The correlation coefficients were found to vary from moderate ($r = 0.58$) to strongest ($r = 0.74$) positive correlation during geomagnetically

quiet conditions while geomagnetically disturbed conditions recorded a weak positive correlation (r = 0.28).

Recommendations

This research presents patterns in the EEJ and EIA strength over East Africa during the solar minimum period. Since EEJ and EIA might influence the occurrence of ionospheric irregularities which in turn lead to scintillations of communication and navigation signals, we recommend simultaneous analysis of EEJ, EIA and scintillation data. This would reveal the influence of EEJ and EIA on the occurrence of scintillations.

It is unclear whether the conclusions drawn over the study area based on data of disturbed geomagnetic conditions can be obtained over other regions. Therefore, we recommend investigations of the correlations between EEJ and EIA during low solar activity and disturbed geomagnetic conditions to be conducted over other regions in the near future.

Acknowledgments

The authors would like to acknowledge the World Data Center, UNAVCO, and INTERMAGNET for donating their free Kp index, GPS data, and daily magnetometer data respectively, for better success of the early planned work.

References

Abadi, P., Saito, S., & Srigutomo, W. (2014). Low-latitude scintillation occurrences around the equatorial anomaly crest over Indonesia. *Annales Geophysicae (09927689)*, *32*(1).

Balan, N., Shiokawa, K., Otsuka, Y., Watanabe, S., & Bailey, G. J. (2009). Super plasma fountain and equatorial ionization anomaly during penetration electric field. *Journal of Geophysical Research: Space Physics*, *114*(A3).

Bolaji, O., Owolabi, O., Falayi, E., Jimoh, E., Kotoye, A., Odeyemi, O., Rabiu, B., Doherty, P., Yizengaw, E., & Yamazaki, Y. (2017). Observations of equatorial ionization anomaly over Africa and Middle East during a year of deep minimum. *Annales Geophysicae*, *35*(1), 123–132.

Chakraborty, S. K., & Hajra, R. (2009). Electrojet control of ambient ionization near the crest of the equatorial anomaly in the Indien zone. *Annales Geophysicae: Atmospheres, Hydrospheres and Space Sciences*, *27*(1), 93.

Chau, J. L., Hoffmann, P., Pedatella, N. M., Matthias, V., & Stober, G. (2015). Upper mesospheric lunar tides over middle and high latitudes during sudden stratospheric warming events. *Journal of Geophysical Research: Space Physics*, *120*(4), 3084–3096.

Dabas, R. S., Singh, L., Lakshmi, D. R., Subramanyam, P., Chopra, P., & Garg, S. C. (2003). Evolution and dynamics of equatorial plasma bubbles: Relationships to ExB drift, postsunset total electron content enhancements, and equatorial electrojet strength. *Radio Science*, *38*(4), 14–1.

Eastes, R. W., Solomon, S. C., Daniell, R. E., Anderson, D. N., Burns, A. G., England, S. L., Martinis, C. R., & McClintock, W. E. (2019). Global-scale observations of the equatorial ionization anomaly. *Geophysical Research Letters*, *46*(16), 9318–9326.

Jose, L., Ravindran, S., Vineeth, C., Pant, T. K., & Alex, S. (2011a). Investigation of the response time of the equatorial ionosphere in context of the equatorial electrojet and equatorial ionization anomaly. *Annales Geophysicae*, *29*(7), 1267–1275.

Jose, L., Ravindran, S., Vineeth, C., Pant, T. K., & Alex, S. (2011b). Investigation of the response time of the equatorial

ionosphere in context of the equatorial electrojet and equatorial ionization anomaly. *Annales Geophysicae*, *29*(7), 1267–1275.

Lühr, H., Alken, P., & Zhou, Y.-L. (2021). The equatorial electrojet. *Ionosphere Dynamics and Applications*, 281–299.

Mungufeni, P., Habarulema, J. B., Migoya-Orué, Y., & Jurua, E. (2018). Statistical analysis of the correlation between the equatorial electrojet and the occurrence of the equatorial ionisation anomaly over the East African sector. *Annales Geophysicae*, *36*(3), 841–853.

Pedatella, N. M., Fuller-Rowell, T., Wang, H., Jin, H., Miyoshi, Y., Fujiwara, H., Shinagawa, H., Liu, H.-L., Sassi, F., & Schmidt, H. (2014). The neutral dynamics during the 2009 sudden stratosphere warming simulated by different whole atmosphere models. *Journal of Geophysical Research: Space Physics*, *119*(2), 1306–1324.

Rabiu, A. B., Folarin, O. O., Uozumi, T., Abdul Hamid, N. S., & Yoshikawa, A. (2017). Longitudinal variation of equatorial electrojet and the occurrence of its counter electrojet. *Annales Geophysicae*, *35*(3), 535–545.

Rastogi, R. G., & Klobuchar, J. A. (1990). Ionospheric electron content within the equatorial F 2 layer anomaly belt. *Journal of Geophysical Research: Space Physics*, *95*(A11), Article A11.

Rush, C. M., Rush, S. V., Lyons, L. R., & Venkateswaran, S. V. (1969). Equatorial anomaly during a period of declining solar activity. *Radio Science*, *4*(9), 829–841.

Schnepf, N. R., Nair, M., Maute, A., Pedatella, N. M., Kuvshinov, A., & Richmond, A. D. (2018). A comparison of model-based ionospheric and ocean tidal magnetic signals with observatory data. *Geophysical Research Letters*, *45*(15), 7257–7267.

Sethia, G., Rastogi, R. G., Deshpande, M. R., & Chandra, H. (1980). Equatorial electrojet control of the low latitude ionosphere. *Journal of Geomagnetism and Geoelectricity*, *32*(4), 207–216.

Venkatesh, K., Fagundes, P. R., Prasad, D. S. V. V. . d., Denardini, C. M., de Abreu, A. J., de Jesus, R., & Gende, M. (2015). Day-to-day variability of equatorial electrojet and its role on the day-to-day characteristics of the equatorial ionization anomaly over the Indian and Brazilian sectors. *Journal of Geophysical Research: Space Physics*, *120*(10), 9117–9131. https://doi.org/10.1002/2015JA021307

Yamazaki, Y., Richmond, A. D., Maute, A., Liu, H.-L., Pedatella, N., & Sassi, F. (2014). On the day-to-day variation of the equatorial electrojet during quiet periods. *Journal of Geophysical Research: Space Physics*, *119*(8), 6966–6980.

Yue, X., Schreiner, W. S., Pedatella, N., Anthes, R. A., Mannucci, A. J., Straus, P. R., & Liu, J.-Y. (2014). Space weather observations by GNSS radio occultation: From FORMOSAT-3/COSMIC to FORMOSAT-7/COSMIC-2. *Space Weather*, *12*(11), Article 11.